

Inhibitor of Cysteine Proteases Is Critical for Motility and Infectivity of *Plasmodium* Sporozoites

Katja E. Boysen,^a Kai Matuschewski^{a,b}

Max Planck Institute for Infection Biology, Parasitology Unit, Berlin, Germany^a; Institute of Biology, Humboldt University, Berlin, Germany^b

ABSTRACT Malaria is transmitted when motile sporozoites are injected into the dermis by an infected female *Anopheles* mosquito. Inside the mosquito vector, sporozoites egress from midgut-associated oocysts and eventually penetrate the acinar cells of salivary glands. Parasite-encoded factors with exclusive vital roles in the insect vector can be studied by classical reverse genetics. Here, we characterized the *in vivo* roles of *Plasmodium berghei* falstatin/ICP (inhibitor of cysteine proteases). This protein was previously suggested to act as a protease inhibitor during erythrocyte invasion. We show by targeted gene disruption that loss of ICP function does not affect growth inside the mammalian host but causes a complete defect in sporozoite transmission. Sporogony occurred normally in *icp*(−) parasites, but hemocoel sporozoites showed a defect in continuous gliding motility and infectivity for salivary glands, which are prerequisites for sporozoite transmission to the mammalian host. Absence of ICP correlates with enhanced cleavage of circumsporozoite protein, in agreement with a role as a protease regulator. We conclude that ICP is essential for only the final stages of sporozoite maturation inside the mosquito vector. This study is the first genetic evidence that an ICP is necessary for the productive motility of a eukaryotic parasitic cell.

IMPORTANCE Cysteine proteases and their inhibitors are considered ideal drug targets for the treatment of a wide range of diseases, including cancer and parasitic infections. In protozoan parasites, including *Leishmania*, *Trypanosoma*, and *Plasmodium*, cysteine proteases play important roles in life cycle progression. A mouse malaria model provides an unprecedented opportunity to study the roles of a parasite-encoded inhibitor of cysteine proteases (ICP) over the entire parasite life cycle. By precise gene deletion, we found no evidence that ICP influences disease progression or parasite virulence. Instead, we discovered that this factor is necessary for parasite movement and malaria transmission from mosquitoes to mammals. This finding in a fast-moving unicellular protozoan has important implications for malaria intervention strategies and the roles of ICPs in the regulation of eukaryotic cell migration.

Received 22 October 2013 Accepted 29 October 2013 Published 26 November 2013

Citation Boysen KE, Matuschewski K. 2013. Inhibitor of cysteine proteases is critical for motility and infectivity of *Plasmodium* sporozoites. *mBio* 4(6):e00874-13. doi:10.1128/mBio.00874-13.

Editor Louis Miller, NIAID/NIH

Copyright © 2013 Boysen and Matuschewski This is an open-access article distributed under the terms of the [Creative Commons Attribution-Noncommercial-ShareAlike 3.0 Unported license](https://creativecommons.org/licenses/by-nc-sa/4.0/), which permits unrestricted noncommercial use, distribution, and reproduction in any medium, provided the original author and source are credited.

Address correspondence to Kai Matuschewski, matuschewski@mpiib-berlin.mpg.de.

The causative agent of malaria, *Plasmodium*, is a parasitic eukaryotic cell that has a complex life cycle and switches between a vertebrate host and an insect vector. A distinct order of alternating intracellular stages, which replicate and form progeny, and extracellular forms, which rapidly invade new target cells, permits life cycle progression and colonization of new hosts. Entry into and exit from host cells are central and tightly coordinated processes to maximize parasite population expansion. Gaining a better understanding of the molecular mechanisms that drive parasite stage conversion can ultimately aid the rational design of new intervention strategies against the most important vector-borne infectious disease.

Cysteine proteases (CPs) are discussed as promising drug targets in malignancies and infectious diseases (1, 2) and mediate several central processes in parasitic protozoa, including *Plasmodium* (3–6). For instance, hemoglobin degradation is essential for parasite growth and survival inside an erythrocyte, a terminally differentiated and minimally equipped host cell. Biochemical and genetic studies have identified at least three CPs of the falcipain

family (7–10). Furthermore, CPs have critical functions for parasite egress from and invasion of their mammalian and insect hosts (4, 11). Early studies demonstrated that parasite invasion of red blood cells can be blocked with inhibitors of CPs (ICPs) (12, 13). These chemical genetic findings could be extended to merozoite egress from erythrocytes (14, 15). In the mosquito vector, experimental genetics have provided evidence of a vital role for a CP in sporozoite egress from oocysts (16). Studies with broad-specificity protease inhibitors identified a critical CP-mediated step in the processing of the major sporozoite surface protein circumsporozoite protein (CSP), which mediates efficient sporozoite invasion of hepatoma cells (17). Together, the available data suggest multiple critical roles for CPs throughout the life cycle in virtually every *Plasmodium* stage conversion event.

The genomes of parasitic protozoa also encode endogenous CP regulators, termed ICPs. The first ICP was identified in the kinetoplastid *Trypanosoma cruzi* and termed chagasin (18). Chagasin is the founding member of the I42 family of ICPs, which was subsequently recognized in a wide range of prokaryotes and eu-

karyotes (19, 20). *T. cruzi* chagasin regulates cruzipain, the major parasite-encoded CP and a key virulence factor (21, 22). ICPs of the I42 family show weak overall homology but a modestly conserved chagasin-like domain. Structural insights into *T. cruzi* chagasin revealed an immunoglobulin-type fold arranged by eight β -strands, which are connected through six loops, three of which are inserted into the active center of the substrate CP, thereby inhibiting its catalytic activity (23, 24).

On the basis of moderate homology with chagasin, chagasin-like ICPs were subsequently identified and characterized in *Plasmodium falciparum* (falstain; PF3D7_0911900; gi: 124506787), *Plasmodium gallinaceum* (PgSES; gi:68521876), *Plasmodium berghei* (PbICP; PBANKA_081300), and *Plasmodium yoelii* (PyICP) (25–28). Biochemical studies have provided evidence of inhibition of the CPs falcipain-2 and falcipain-3 by falstain, and antibody-mediated inhibition suggested a role for falstain in the facilitation of erythrocyte invasion (25). Similarly, two *Toxoplasma gondii* ICPs or toxostains inhibit the clan CA, family C1 CPs cathepsins B and L at nanomolar concentrations (29).

Sporozoite expression of ICP was initially described in *P. gallinaceum*, a bird malaria parasite (26). While it was incidentally isolated in a salivary gland sporozoite cDNA library, the authors showed that PgSES/ICP is expressed in various stages of the *Plasmodium* life cycle, including asexual blood-stage parasites and mature, i.e., hemocoel and salivary gland-associated, sporozoites. Notably, PgSES is a surface-expressed protein displaying an intriguing spiral-like pattern. These findings were subsequently confirmed in murine malaria parasites (27, 28). *P. berghei* ICP is secreted by salivary gland sporozoites and was suggested to be important for hepatocyte invasion and inhibition of host cell apoptosis (27).

Interestingly, some prokaryotes, such as *Pseudomonas aeruginosa*, apparently lack endogenous CPs despite the presence of an ICP (19), and in *Leishmania*, CPs and ICPs do not colocalize (30). These findings indicate that ICPs may also play additional roles, for instance, in host-pathogen interaction. Null mutants of *Leishmania mexicana* show normal infectivity of macrophages *in vitro* but reduced infectivity to mice (30), and overexpression of chagasin in *T. cruzi* led to reduced infectivity *in vitro* and impaired the capacity to differentiate into trypomastigotes (31).

No experimental genetic data are available yet for apicomplexan parasites. Two studies have proposed vital roles for asexual blood-stage growth (27, 28), a notion that is supported by ICP expression in asexual blood-stage parasites (26, 27). To test this view and potentially validate ICP as a druggable target for antimalarial intervention strategies, we used reverse genetics to select for *icp(-)* parasites in infected mice. We unequivocally show that *P. berghei* ICP is dispensable in blood infection *in vivo* but necessary for continuous sporozoite gliding motility and, as a consequence, for parasite transmission from a mosquito to a mammalian host.

RESULTS

Targeted disruption of *P. berghei* ICP. We initiated our study with a reverse genetic approach and attempted to delete PbICP (Fig. 1A). To this end, we transfected PbANKA parasites with a standard replacement vector and were able to recover recombinant *icp(-)* blood-stage parasites. After *in vivo* cloning through limiting dilution, we obtained a clonal *icp(-)* line, as confirmed by genotyping via diagnostic PCR (Fig. 1B). As independent con-

firmation of successful PbICP deletion, we verified the absence of PbICP transcripts in *icp(-)* parasites by reverse transcription (RT)-PCR of cDNA (Fig. 1C). In these knockout (KO) parasites, the green fluorescent protein (GFP) marker is under the control of the endogenous PbICP promoter (Fig. 1A). In asexual blood-stage parasites, we observed moderate live GFP expression (Fig. 1D).

To further corroborate our findings and facilitate parasite imaging, we generated a second KO line through the transfection of a fluorescent parasite line (32) with our PbICP replacement vector, followed by *in vivo* cloning of *icp(-)*-GFP parasites (Fig. 1B and C). These parasites show constitutive GFP expression under the control of the elongation factor 1 alpha (EF1 α) promoter (Fig. 1D). Southern blot analysis of the genomic DNA (gDNA) of both *icp(-)* and *icp(-)*-GFP parasite lines provided additional proof of the successful replacement of PbICP (see Fig. S1 in the supplemental material). Together, our results unequivocally show that PbICP is not essential in blood-stage parasites.

Asexual blood-stage parasite growth and virulence are not affected by ablation of PbICP. We next studied whether blood infection is modulated in the absence of PbICP. We infected outbred NMRI (Naval Medical Research Institute) mice ($n = 5$) with 10,000 *icp(-)* or wild-type (WT) blood-stage parasites and enumerated their parasitemia (Fig. 1E). This analysis revealed that patency, the time until parasite detection in the peripheral blood, was slightly prolonged in *icp(-)* parasite-infected mice. However, once a blood-stage parasite infection was established, the growth ratios of WT and KO parasites were indistinguishable. We corroborated this finding by the infection of inbred C57BL/6 mice ($n = 5$) with 1,000 infected erythrocytes (Fig. 1E). Again, kinetics and endpoint parasitemia were similar in *icp(-)* and WT parasite-infected mice, despite a minor delay in patency observed in *icp(-)* parasite-infected mice.

To test virulence, we monitored infected C57BL/6 mice for signature symptoms of experimental cerebral malaria (ECM) (Fig. 1F). Similar to mice infected with WT parasites, all of the mice infected with *icp(-)* parasites developed ECM symptoms on day 7 or 8 after infection. In conclusion, ablation of PbICP does not affect either parasite virulence or asexual growth.

***icp(-)* sporozoites fail to colonize mosquito salivary glands.** We next monitored the life cycle progression of *icp(-)* parasites and allowed *Anopheles stephensi* mosquitoes to feed on *icp(-)* parasite-infected mice. Two weeks later, we could detect abundant *icp(-)* oocysts in the mosquitoes' midguts (Fig. 2A), which is indicative of normal ookinete formation and subsequent transformation and growth during sporogony. In marked contrast, we failed to detect *icp(-)* sporozoites in their salivary glands (Fig. 2A). Since this could be due to either failure to form mature sporozoites or a sporozoite-specific defect, we monitored sporozoites in the hemocoels of infected mosquitoes, e.g., in wing veins, by live microscopy (Fig. 2B). We consistently detected WT and *icp(-)* mutant sporozoites, a finding that was corroborated by the quantification of midgut- and hemocoel-associated sporozoites (Fig. 2C). Only salivary gland-associated *icp(-)* sporozoites were markedly decreased to very low numbers. Taken together, the findings show that PbICP is essential for the successful colonization of mosquito salivary glands.

Ablation of PbICP results in impaired gliding motility of hemocoel sporozoites. To gain a better understanding of the developmental arrest of sporozoites, we next tested whether *icp(-)* hemocoel sporozoites were viable and exhibited normal parasite

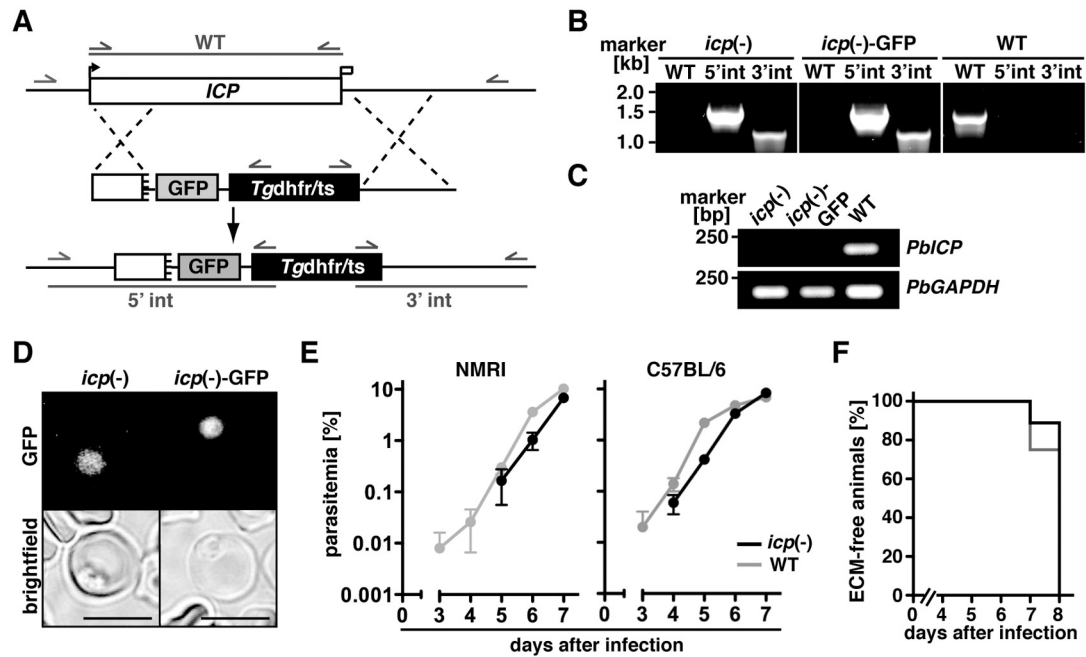


FIG 1 PbICP is not essential for asexual *P. berghei* blood infection. (A) Replacement strategy used to generate the *icp(-)* and *icp(-)-GFP* parasite lines. The WT PbICP locus was targeted with a linearized replacement plasmid containing a 5' fragment and the 3' untranslated region of PbICP flanking GFP and the positive selection marker *T. gondii dhfr/ts* (*Tgdhfr/ts*). After double-crossover homologous recombination, exon 2 of the PbICP open reading frame was replaced with GFP and the selection marker, resulting in the loss-of-function *icp(-)* allele. Replacement- and WT-specific test primer combinations and expected PCR fragments are shown as arrows and lines, respectively. int, integration. (B) Confirmation of PbICP gene disruption by replacement-specific PCR analysis. The diagnostic primer combinations amplify a signal in the recombinant locus only (5' int, 3' int). Two independent clonal *icp(-)* lines, *icp(-)* and *icp(-)-GFP*, were generated after the successful transfection of parasite strains PbANKA and PbANKA_GFP, respectively. The absence of a WT-specific signal in the KO parasites confirms the purity of the clonal populations. (C) Absence of PbICP transcripts in *icp(-)* and *icp(-)-GFP* parasites (top panel). Shown is an RT-PCR analysis of cDNA generated from RNA of *icp(-)*, *icp(-)-GFP*, and WT blood-stage parasites. PbGAPDH transcripts were amplified as a control (bottom). (D) Live imaging of *icp(-)* (left) and *icp(-)-GFP* (right) parasites. Shown are fluorescent images of *icp(-)* and *icp(-)-GFP* trophozoites. Note that GFP expressed under the control of the PbICP promoter [*icp(-)*] is only slightly less bright than in the reference strain, where GFP is expressed under the control of the EF1 α promoter [*icp(-)-GFP*]. Scale bars, 5 μ m. (E) Growth rates of *icp(-)* (black circles) and WT (gray circles) parasites in outbred NMRI mice (left) and inbred C57BL/6 mice (right) ($n = 5$ each). Female NMRI mice were infected with 10,000 *icp(-)* iRBCs, and female C57BL/6 mice were infected with 1,000 WT iRBCs. The values shown are means \pm the standard errors of the means. Note that *icp(-)* parasite-infected mice showed a slight delay in the onset of parasitemia after infection. Parasitemia was monitored by daily microscopic examination of Giemsa-stained blood films. (F) Kaplan-Meier analysis of signature symptoms of ECM in C57BL/6 mice infected with 10,000 *icp(-)* (black line) or WT (gray line) parasites.

locomotion, termed gliding motility (33, 34). In an initial experiment, we monitored the live motility of freshly isolated hemocoel sporozoites (Fig. 3A). While we could assign the characteristic continuous circular locomotion to a substantial proportion (~18%) of WT hemocoel sporozoites, we failed to detect this capacity in any of the *icp(-)* sporozoites analyzed. To further corroborate this finding, we allowed hemocoel sporozoites to glide on glass slides and then used an immunofluorescence assay with an anti-CSP antibody to detect the signature trails of motile sporozoites (Fig. 3B). In good agreement with our live-microscopy data, we found circular trails in ~20% of the WT sporozoites but only ~3% of the *icp(-)* sporozoites. Moreover, compared to WT hemocoel sporozoites, the number of completed circles made by *icp(-)* sporozoites was considerably lower and the shape of the trails was irregular (Fig. 3B). A substantial fraction (~18%) of *icp(-)* hemocoel sporozoites displayed very short trails, indicative of aberrant and nonproductive motility. We conclude that *icp(-)* hemocoel sporozoites are viable and motile. However, continuous and extended gliding motility is lost upon the targeted deletion of PbICP, providing a plausible explanation for the observed defect in salivary gland colonization.

Role of PbICP in processing of CSP. Several sporozoite proteins have been identified as important for salivary gland invasion (for reviews, see references 34 and 35). The most prominent proteins are CSP and thrombospondin-related anonymous protein (TRAP). Both of these proteins are proteolytically processed and shed during sporozoite gliding (17, 36). These processes can be inhibited by CP and serine protease inhibitors, respectively. CSP is synthesized as an ~54-kDa precursor that is proteolytically processed to a mature ~44-kDa protein as the sporozoite matures (37). We hypothesized that ablation of PbICP might result in deregulation of the timely proteolytic processing of CSP, but not TRAP.

We first performed Western blot analysis by using an anti-CSP antibody and midgut or hemocoel sporozoites (Fig. 4A). We detected both forms of CSP in WT and *icp(-)* sporozoites. As expected (37), the processed form was less prominent in WT midgut sporozoites than in hemocoel sporozoites. Intriguingly, the amount of the processed form of CSP was increased in *icp(-)* midgut sporozoites, resembling the state in WT hemocoel sporozoites. We next quantified the ratio of mature to precursor CSP (Fig. 4B). In *icp(-)* midgut sporozoites, CSP processing was sig-

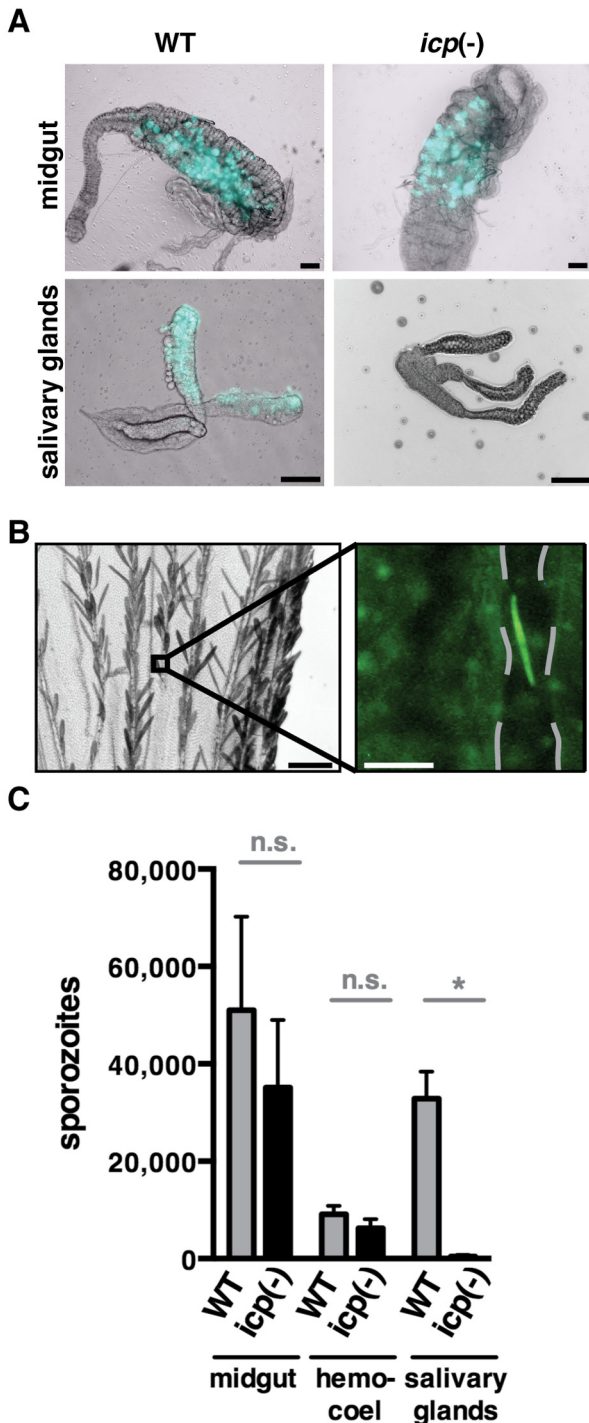


FIG 2 PbICP is essential for the successful colonization of salivary glands. (A) Live-microscopy images of mosquito midguts colonized with mature WT or *icp(-)* oocysts (top) and the corresponding salivary glands (bottom). No *icp(-)* sporozoites could be detected in salivary glands of infected mosquitoes, while WT sporozoites were abundant. Bars, 100 μm. (B) Detection of *icp(-)* sporozoites in the mosquito hemocoel. Shown is a representative live-microscopy image of an *icp(-)* sporozoite in a mosquito wing vein, outlined by a dashed line (right side; bar, 10 μm). The imaged area is boxed in the lower-magnification bright-field image (left side; bar, 100 μm). (C) Numbers of sporozoites in the midguts, hemocoels, and salivary glands of WT (gray columns) and *icp(-)* (black columns) sporozoite-infected *A. stephensi* mosquitoes. Sporozoites of each parasite line were enumerated in four independent experiments. Sporozoites of each parasite line were enumerated in four independent experiments. Sporozoites of each parasite line were enumerated in four independent experiments. Sporozoites of each parasite line were enumerated in four independent experiments. (Continued)

nificantly enhanced compared to that in WT midgut sporozoites. The proportion of the mature form of CSP was further increased in either *icp(-)* or WT hemocoel sporozoites (Fig. 4B). Additional nonparametric Kruskal-Wallis analysis confirmed a significantly higher proportion of the CSP precursor in WT midgut sporozoites ($P < 0.05$). In comparison, TRAP processing was not altered in the absence of PbICP and comparable in midgut and hemocoel sporozoites of both parasite populations (see Fig. S2 in the supplemental material). Together, these data show that ablation of PbICP correlates with premature CSP cleavage in immature midgut sporozoites, which is indicative of dysregulation of sporozoite maturation.

We next quantified CSP shedding into trails deposited by WT and *icp(-)* midgut sporozoites (Fig. 5A). In good agreement with our observation of increased CSP cleavage in *icp(-)* sporozoites, significantly more *icp(-)* than WT midgut sporozoites were found to deposit CSP trails (Fig. 5B). Although we occasionally observed extended trails in *icp(-)* midgut sporozoites (see Fig. S3 in the supplemental material), as we did in WT parasites, the mean trail lengths of WT and *icp(-)* sporozoites that deposited CSP into the trails were indistinguishable (Fig. 5B). Despite these signs of motility, intravenous injection into C57BL/6 mice confirmed the immaturity of both WT and *icp(-)* midgut sporozoites, which typically fail to establish a blood infection (see Fig. S4).

PbICP is essential for hepatocyte infection. We finally explored the ability of *icp(-)* hemocoel sporozoites to infect hepatocytes (Fig. 6A). We found 20% of the WT but none of the *icp(-)* sporozoites to have invaded hepatoma cells. In good agreement, when we intravenously injected 1,000 hemocoel sporozoites into susceptible C57BL/6 mice, only WT sporozoites consistently caused a blood-stage parasite infection (Fig. 6B).

Together, our data establish that PbICP is essential for continuous gliding locomotion of hemocoel sporozoites and, as a likely consequence, for salivary gland invasion and parasite transmission from an insect to a mammalian host.

DISCUSSION

The most important finding of our study is that PbICP is necessary for sporozoite motility and dispensable for blood infection *in vivo*. Results of previous studies anticipated a vital role(s) for PbICP in blood-stage parasite development. PbICP is expressed in blood-stage *P. gallinaceum* and *P. berghei* parasites (26, 27). In *P. falciparum*, falstatin/PfICP was detected in rings and schizonts, but not in trophozoites, and inhibition of falstatin with specific antibodies blocked erythrocyte invasion *in vitro* (25). Moreover, one study postulated that PyICP is likely to be essential in blood-stage parasites (28). Our experimental genetic data on *P. berghei*, the most widely used murine malaria model (38), reject this conclusion. In two independent transfection experiments, we could delete PbICP from a blood-stage population and found no evidence of significant defects in either parasite growth or virulence *in vivo*.

It is plausible that a severe defect in erythrocyte invasion, erythrocyte rupture, and/or subsequent egress of merozoites, as sug-

Figure Legend Continued

gent experiments. Note that the numbers of hemocoel-associated sporozoites are similar in WT and *icp(-)* parasite-infected mosquitoes, while salivary glands are successfully invaded by WT but not *icp(-)* sporozoites. The values shown are means \pm the standard errors of the means. n.s., nonsignificant. *, $P < 0.05$ (Mann-Whitney test).

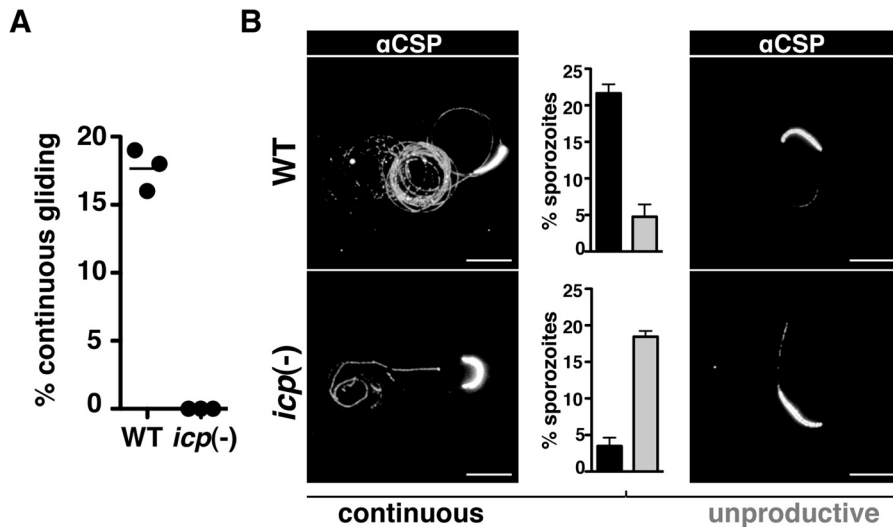


FIG 3 Gliding locomotion is severely impaired in *icp(-)* hemocoel sporozoites. (A) Live monitoring of gliding locomotion in hemocoel sporozoites. A substantial proportion (~18%) of the WT, but not the *icp(-)*, hemocoel sporozoites performed circular and continuous gliding motility within a time frame of ~15 min. Each dot indicates the percentage of gliding sporozoites ($n = 100$ per parasite line and experiment). (B) Immunofluorescence assay of WT and *icp(-)* hemocoel sporozoites. Sporozoites were allowed to glide for 1 h, fixed, and stained with an anti-CSP antibody (α CSP). About 20% of the WT and ~3% of the *icp(-)* sporozoites deposited circular trails onto glass slides (black columns). Note that *icp(-)* hemocoel sporozoites produced only a few irregular circles. Noncircular trails, termed unproductive, were detected in ~5% of the WT and ~18% of the *icp(-)* sporozoites (gray columns) ($n = 300$ each). Bars, 10 μ m.

gested for falstatin (25) and one of its targets, falcipain-2 (39, 40), would have impaired parasite population expansion in infected mice. We cannot exclude the possibility that the importance of ICP in these key processes during blood infection differs among various *Plasmodium* species. Although all of the studies reported thus far concur on the blood-stage expression of ICP, distinct ICP localization in sporozoites, ranging from deposition of PbICP onto trails (27) to a unique striped pattern of PgICP/SES (26), indicates specifications in different *Plasmodium* species. A systematic gene deletion and complementation analysis of PbICPs and their corresponding CPs in related *Plasmodium* parasites is clearly warranted and might represent an informative example of shared and/or unique roles for PbICP and CP across *Plasmodium* parasites.

On the basis of our phenotypic analysis of *icp(-)* sporozoites, we hypothesize that all of the *Plasmodium* ICPs play roles essential

for mosquito-to-vertebrate transmission. Herein, we report that PbICP is a critical factor for three crucial traits of sporozoite transmission, i.e., (i) continuous, and thereby productive, gliding motility; (ii) salivary gland invasion; and (iii) hepatocyte invasion. We could readily detect *icp(-)* sporozoites in hemocoel preparations and *in vivo* in the hemolymph-filled veins of mosquito wings. These data show that neither sporogony nor sporozoite egress from oocysts was impaired. While sporozoites typically reach their final target organ, the salivary glands, through passive circulation in the mosquito hemocoel, it has been proposed that this journey is reinforced by active sporozoite gliding along the basal lamina that surrounds both the midgut and the salivary glands (33, 41). The observed lack of continuous gliding locomotion in *icp(-)* sporozoites correlates with a failure to colonize the salivary glands, despite their abundant presence throughout the mosquito body cavities filled with hemolymph.

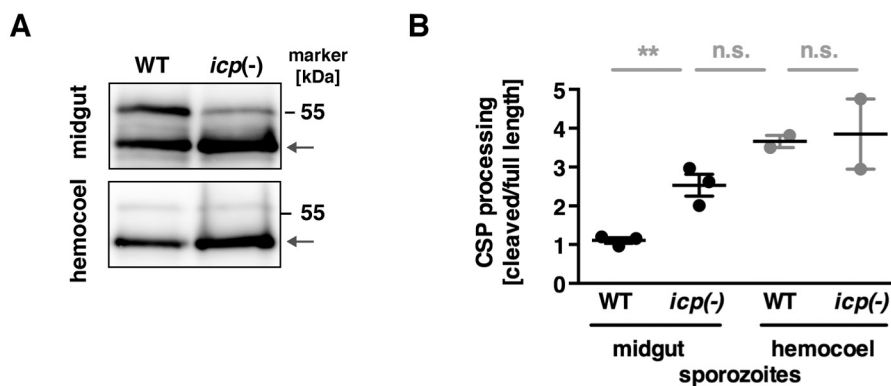


FIG 4 Enhanced processing of CSP in *icp(-)* midgut sporozoites. (A) Representative Western blot assay showing precursor and proteolytically processed forms (arrow) of CSP from midgut (top) and hemocoel (bottom) sporozoites. CSP processing is enhanced in *icp(-)* midgut sporozoites and resembles WT hemocoel sporozoites. (B) Quantification of proteolytic cleavage of CSP in midgut and hemocoel sporozoites. The mean gray value per area was quantified and is presented as the ratio of cleaved to full-length CSP. Shown are mean ratios \pm the standard errors of the means. **, $P < 0.01$; n.s., nonsignificant (unpaired t test).

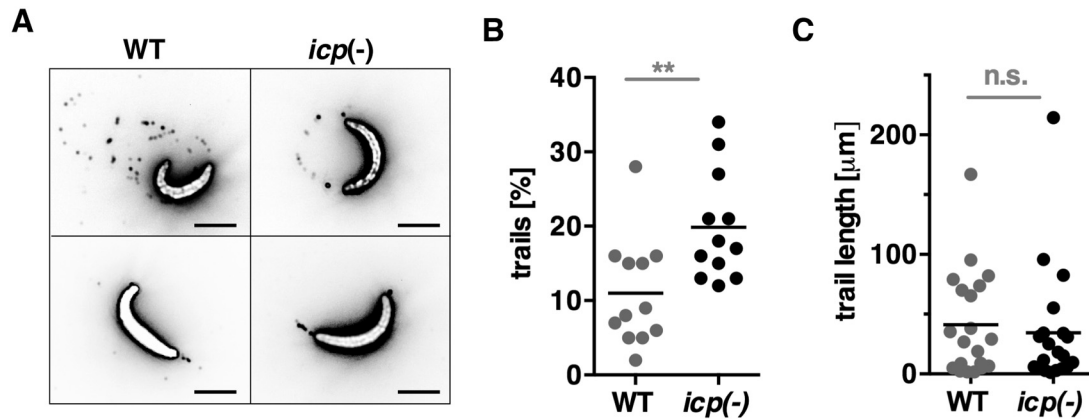


FIG 5 Higher proportion of CSP-positive trails in *icp(-)* midgut sporozoites. (A) Representative immunofluorescence micrographs of midgut sporozoites of WT and *icp(-)* parasites. Bars, 5 μm. (B) Proportions of WT (gray dots) and *icp(-)* (black dots) midgut sporozoites with CSP-positive trails. **, $P < 0.01$ (Mann-Whitney test). (C) Quantification of trail lengths of WT (gray dots) and *icp(-)* (black dots) sporozoites ($n = 20$ each). n.s., nonsignificant (Mann-Whitney test).

For successful salivary gland invasion and subsequent transmission to a mammalian host, sporozoites first attach to receptors on the basal side of acinar cells (35, 42, 43). Next, they penetrate the basal lamina surrounding the salivary gland, traverse the secretory cells, and finally enter the secretory cavity, from where they have access to the secretory duct (41, 44, 45). Using live microscopy, we failed to detect any sporozoites inside salivary glands, either in the cytoplasm of acinar cells or in the secretory cavity. This finding strongly indicates that the defect in *icp(-)* sporozoites likely occurs during recognition and attachment to salivary gland receptors.

Intriguingly, we observed enhanced cleavage of CSP, but not TRAP, in good agreement with previous studies that showed inhibition of precursor processing by CP and serine protease inhibitors, respectively (17, 36). We propose that ICP regulates the CP-dependent processing of CSP, which in turn results in impaired gliding locomotion. Absence of PbICP resulted in a complete block of hepatocyte invasion *in vitro* and *in vivo*. This addi-

tional role of ICP is in good agreement with antibody inhibition experiments (27). However, this defect might be a direct consequence of ablated gliding motility. The multiple defects seen in *icp(-)* sporozoites are consistent with the key roles of additional sporozoite proteins, including sporozoite-specific protein 6 and sporozoite invasion-associated protein 1 (46, 47). Similar to ICP, these surface proteins are critical factors in salivary gland colonization, hepatocyte invasion, and gliding locomotion and could be additional targets of proteolytic processing.

Immunoprofiling with a protein microarray identified PfICP/falstatin as an antigen that is recognized in immune serum samples obtained both from regions where malaria is hyperendemic and after immunization with radiation-attenuated sporozoites (48). This finding strongly suggests that ICP continues to be shed from sporozoites in the vertebrate host. Although we provide compelling evidence that PbICP is not a key virulence factor for *Plasmodium* blood-stage parasites, the vital role(s) in sporozoite locomotion and hepatocyte invasion together with its regulatory

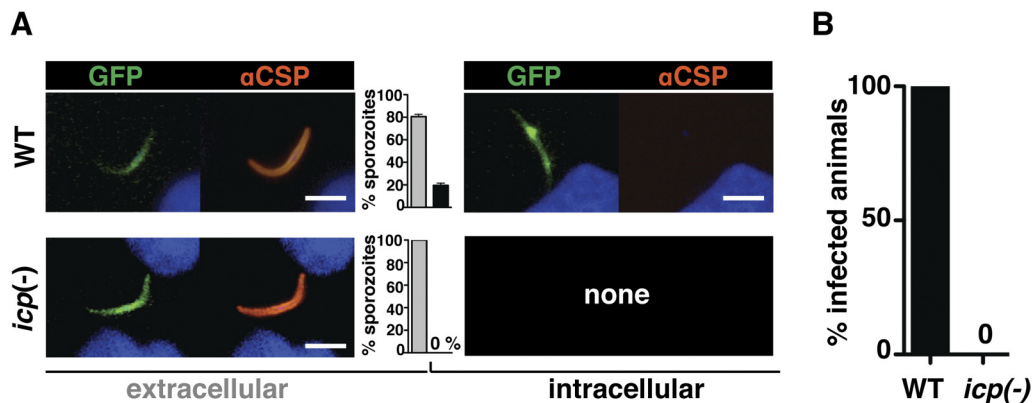


FIG 6 *icp(-)* hemocoel sporozoites are noninfectious *in vitro* and *in vivo*. (A) Shown is a dual-color assay to assess the *in vitro* infectivity of hemocoel sporozoites for cultured hepatoma cells. Sporozoites expressed GFP under the control of the constitutive EF1α promoter. Extracellular sporozoites were detected with an anti-*P. berghei* CSP antibody (red) and displayed green fluorescence (left), while intracellular parasites were GFP positive only (right). Graphs (center) show the enumeration of cell invasion ($n = 100$ each, done in duplicate). Note that ~20% of the WT hemocoel sporozoites were found to be intracellular (black columns), while all of the *icp(-)* sporozoites remained extracellular (gray columns). Bars, 5 μm. (B) *In vivo* infectivity of sporozoites for C57BL/6 mice. One thousand hemocoel sporozoites were injected intravenously and blood-stage parasite infection was monitored by daily microscopic examination of Giemsa-stained blood smears ($n = 4$ each). The patency of WT sporozoite-infected mice was 4 days.

role in CSP processing, reported herein, fully support the candidacy of PfICP for subunit-based antimalarial vaccine strategies. Indeed, the only advanced malaria vaccine, which is currently undergoing phase 3 evaluation, RTS,S/AS01E, consists of a portion of *P. falciparum* CSP (49–51). It is tempting to hypothesize that lasting humoral and cellular immunogenicity of CSP might be augmented by the inclusion of candidate regulators, such as ICP described herein, into a second-generation antipreerythrocytic vaccine.

In conclusion, our experimental genetic analysis identified a key role for a *Plasmodium* ICP in sporozoite motility and infectivity. Together with robust recognition during naturally acquired immunity to malaria, our findings provide a rationale for the development of ICP-based intervention strategies that target infection of the vertebrate host, one critical bottleneck in the *Plasmodium* life cycle.

MATERIALS AND METHODS

Experimental animals. All of the animal work in this study was conducted in accordance with the German animal protection act of 18 May 2006 (BGBl. I S. 1207), which implements directive 86/609/EEC of the European Union and the European Convention for the protection of vertebrate animals used for experimental and other scientific purposes. The protocol was approved by the ethics committee of the Max Planck Institute for Infection Biology and the Berlin state authorities (LAGeSo registration no. G0469/09). The animals used were from Charles River Laboratories.

Parasite transfection and genotypic analysis. For disruption of PbICP, two fragments were amplified by using primers 5' KO_flank_for and 5' KO_flank_rev to obtain the 5' fragment and 3' KO_flank_for and 3' KO_flank_rev for the 3' fragment with *P. berghei* gDNA as the template. Both fragments were cloned into *P. berghei* transfection vector b3D, resulting in targeting plasmid pICP. This targeting plasmid was linearized with SacII and KpnI, and parasite transfection, positive selection, and parasite cloning were performed as described previously (32). Genotyping of recombinant parasite populations was performed by PCR with integration- and WT-specific primers. The genotype of the two selected *icp*(-) parasite populations was confirmed by Southern blot analysis with the PCR DIG probe synthesis kit and the DIG luminescence detection kit (Roche) according to the manufacturer's protocol. For amplification of the hybridization probe, primers 5' KO_flank_for and 5' KO_flank_rev were used. The hybridization probe was annealed to blots of agarose gel-separated HindIII- and HindIII/NdeI-digested gDNA, resulting in bands of 7.7 and 1.9 kb, respectively, for *icp*(-) sporozoites and 2.9 kb each for WT sporozoites. For RT-PCR analysis, we isolated poly(A⁺) RNA with oligo(dT) columns (Invitrogen). For cDNA synthesis and amplification, we performed a two-step PCR with oligo(dT) primers (Ambion) and subsequent standard PCRs with primers PbICP_for and PbICP_rev and primers GAPDH_for and GAPDH_rev. All of the primers used are listed in Table S1 in the supplemental material.

Analysis of parasite development. *A. stephensi* mosquito rearing and maintenance were carried out under a 14-h light/10-h dark cycle, at 75% humidity, and at 28 or 20°C, respectively. Blood-stage parasite development was analyzed *in vivo* in asynchronous infections with NMRI or C57BL/6 mice. Gametocyte differentiation and exflagellation of microgametes were detected in mice before ookinete culture or mosquito feeding, respectively. Sporozoites were dissected and analyzed as described previously (52). Briefly, for the collection of midgut sporozoites, the midguts of infected mosquitoes were dissected and gently ground in a test tube with a loosely fitting microhomogenizer to free the sporozoites. The sporozoite suspension was centrifuged at 20 × *g* for 3 min to remove mosquito tissue debris. After an additional washing, the sporozoite-containing supernatants were pooled. To collect hemocoel sporozoites, the last abdominal segment of mosquitoes was removed with fine needles.

Subsequently, the membranous postspiracular area of the mesothorax was punctured with a fine glass needle and the abdominal hemocoel was gently perfused with 10 μl of RPMI 1640. Hemocoel sporozoites were isolated on days 15 to 26 after infection. For salivary gland sporozoites, infected mosquitoes were dissected and the pooled salivary glands were ground and processed as described for the midgut sporozoites. The numbers of sporozoites in the respective tissues were determined with a hemocytometer.

Sporozoite gliding motility. Eight-well glass slides were precoated with RPMI medium containing 3% bovine serum albumin (BSA) for 20 min at 37°C in a humid chamber. Sporozoites were dissected in RPMI–3% BSA and incubated for 60 min at 37°C for settlement and gliding. After fixation with 4% paraformaldehyde, sporozoites and trails were detected with an anti-*P. berghei* CSP antibody (53).

Sporozoite invasion assay. To determine host cell invasion, the protocol was slightly modified from the established two-color invasion assay (54). Briefly, WT (GFPcon) and *icp*(-)-GFP sporozoites were added to cultured hepatoma (Huh7) cells and incubated for 1 h at 37°C. Parasites were then fixed and stained with anti-CSP antibody without previous permeabilization. As a result, CSP will be detectable on extracellular sporozoites but not on intracellular sporozoites that have successfully invaded hepatoma cells. Constitutive expression of GFP allowed the detection of both extracellular and intracellular parasites.

Western blot analysis. Protein samples were analyzed by SDS-PAGE and electrophoretically transferred to polyvinylidene difluoride membranes. For the detection of CSP and TRAP processing in WT and *icp*(-) sporozoites, midgut and hemocoel sporozoites were isolated, resuspended in 10 μl of SDS sample buffer, and incubated for 5 min at 95°C. Blotted membranes were probed with antibodies to *P. berghei* TRAP and CSP (53, 55), and bound antibody was detected with horseradish peroxidase-coupled goat anti-mouse and anti-rabbit IgG, respectively, and developed with ECL (GE Healthcare, Freiburg, Germany). To calculate the ratio of mature to precursor CSP, we measured the mean gray values of CSP signals on midgut- and hemocoel-associated sporozoites (*n* = 3 and 2, respectively) with ImageJ (<http://rsb.info.nih.gov/ij/>).

Murine infections. Female C57BL/6 or NMRI mice were infected with 1,000 or 10,000 infected red blood cells (iRBCs), respectively, in RPMI medium. iRBCs were injected intravenously into the tail vein. To test the infectivity of hemocoel and midgut sporozoites, 1,000 and 10,000 sporozoites, respectively, were injected intravenously into the tail veins of C57BL/6 mice. Patency, i.e., the time to the detection of blood-stage parasites, and parasitemia were determined by daily microscopic examination of Giemsa-stained blood films. During the analysis, the development of signature symptoms of ECM was monitored in C57BL/6 mice. Mice were diagnosed with onset of ECM if they showed behavioral and functional abnormalities, such as ataxia, paralysis, or convulsions. Mice were sacrificed immediately after a diagnosis of ECM.

Statistical analysis. Statistical significance was assessed by using the Mann-Whitney test, Student's *t* test, or Kruskal-Wallis analysis, with a *P* value of <0.05 considered a significant difference. All of the statistical tests were computed with GraphPad Prism 5 (GraphPad Software).

SUPPLEMENTAL MATERIAL

Supplemental material for this article may be found at <http://mbio.asm.org/lookup/suppl/doi:10.1128/mBio.00874-13/-/DCSupplemental>.

Figure S1, TIF file, 0.4 MB.

Figure S2, TIF file, 0.5 MB.

Figure S3, TIF file, 0.3 MB.

Figure S4, TIF file, 0.2 MB.

Table S1, PDF file, 0.1 MB.

ACKNOWLEDGMENTS

This work was supported by the Max Planck Society and in part by the European Commission (EviMalaR no. 34).

REFERENCES

- Palermo C, Joyce JA. 2008. Cysteine cathepsin proteases as pharmacological targets in cancer. *Trends Pharmacol. Sci.* 29:22–28.
- Turk B. 2006. Targeting proteases: successes, failures and future prospects. *Nat. Rev. Drug Discov.* 5:785–799.
- Rosenthal PJ. 2004. Cysteine proteases of malaria parasites. *Int. J. Parasitol.* 34:1489–1499.
- Rosenthal PJ. 2011. Falcipains and other cysteine proteases of malaria parasites. *Adv. Exp. Med. Biol.* 712:30–48.
- Sajid M, Robertson SA, Brinen LS, McKerrow JH. 2011. Cruzain: the path from target validation to the clinic. *Adv. Exp. Med. Biol.* 712:100–115.
- Teixeira C, Gomes JR, Gomes P. 2011. Falcipains, *Plasmodium falciparum* cysteine proteases as key drug targets against malaria. *Curr. Med. Chem.* 18:1555–1572.
- Sijwali PS, Rosenthal PJ. 2004. Gene disruption confirms a critical role for the cysteine protease falcipain-2 in hemoglobin hydrolysis by *Plasmodium falciparum*. *Proc. Natl. Acad. Sci. U. S. A.* 101:4384–4389.
- Hogg T, Nagarajan K, Herzberg S, Chen L, Shen X, Jiang H, Wecke M, Blohmke C, Hilgenfeld R, Schmidt CL. 2006. Structural and functional characterization of falcipain-2, a hemoglobinase from the malarial parasite *Plasmodium falciparum*. *J. Biol. Chem.* 281:25425–25437.
- Drew ME, Banerjee R, Uffman EW, Gilbertson S, Rosenthal PJ, Goldberg DE. 2008. Plasmodium food vacuole plasmepsins are activated by falcipains. *J. Biol. Chem.* 283:12870–12876.
- Chugh M, Sundararaman V, Kumar S, Reddy VS, Siddiqui WA, Stuart KD, Malhotra P. 2013. Protein complex directs hemoglobin-to-hemozoin formation in *Plasmodium falciparum*. *Proc. Natl. Acad. Sci. U. S. A.* 110:5392–5397.
- Blackman MJ. 2008. Malarial proteases and host cell egress: an “emerging” cascade. *Cell. Microbiol.* 10:1925–1934.
- Banyal HS, Misra GC, Gupta CM, Dutta GP. 1981. Involvement of malarial proteases in the interaction between the parasite and host erythrocyte in *Plasmodium knowlesi* infections. *J. Parasitol.* 67:623–626.
- Hadley T, Aikawa M, Miller LH. 1983. *Plasmodium knowlesi*: studies on invasion of rhesus erythrocytes by merozoites in the presence of protease inhibitors. *Exp. Parasitol.* 55:306–311.
- Salmon BL, Oksman A, Goldberg DE. 2001. Malaria parasite exit from the host erythrocyte: a two-step process requiring extraerythrocytic proteolysis. *Proc. Natl. Acad. Sci. U. S. A.* 98:271–276.
- Wickham ME, Culvenor JG, Cowman AF. 2003. Selective inhibition of a two-step egress of malaria parasites from the host erythrocyte. *J. Biol. Chem.* 278:37658–37663.
- Aly AS, Matuschewski K. 2005. A malarial cysteine protease is necessary for *Plasmodium* sporozoite egress from oocysts. *J. Exp. Med.* 202:225–230.
- Coppi A, Pinzon-Ortiz C, Hutter C, Sinnis P. 2005. The *Plasmodium* circumsporozoite protein is proteolytically processed during cell invasion. *J. Exp. Med.* 201:27–33.
- Monteiro AC, Abrahamson M, Lima AP, Vannier-Santos MA, Scharfstein J. 2001. Identification, characterization, and localization of chagasin, a tight-binding cysteine protease inhibitor in *Trypanosoma cruzi*. *J. Cell Sci.* 114:3933–3942.
- Rigden DJ, Mosolov VV, Galperin MY. 2002. Sequence conservation in the chagasin family suggests a common trend in cysteine proteinase binding by unrelated protein inhibitors. *Protein Sci.* 11:1971–1977.
- Sanderson SJ, Westrop GD, Scharfstein J, Mottram JC, Coombs GH. 2003. Functional conservation of a natural cysteine peptidase inhibitor in protozoan and bacterial pathogens. *FEBS Lett.* 542:12–16.
- Engel JC, Doyle PS, Hsieh I, McKerrow JH. 1998. Cysteine protease inhibitors cure an experimental *Trypanosoma cruzi* infection. *J. Exp. Med.* 188:725–734.
- Alvarez VE, Niemirowicz GT, Cazzulo JJ. 2012. The peptidases of *Trypanosoma cruzi*: digestive enzymes, virulence factors, and mediators of autophagy and programmed cell death. *Biochim. Biophys. Acta* 1824:195–206.
- Wang SX, Pandey KC, Scharfstein J, Whisstock J, Huang RK, Jacobelli J, Fletterick RJ, Rosenthal PJ, Abrahamson M, Brinen LS, Rossi A, Sali A, McKerrow JH. 2007. The structure of chagasin in complex with a cysteine protease clarifies the binding mode and evolution of an inhibitor family. *Structure* 15:535–543.
- Figueiredo da Silva AA, de Carvalho Vieira L, Krieger MA, Goldenberg S, Zanchin NI, Guimarães BG. 2007. Crystal structure of chagasin, the endogenous cysteine-protease inhibitor from *Trypanosoma cruzi*. *J. Struct. Biol.* 157:416–423.
- Pandey KC, Singh N, Arastu-Kapur S, Bogyo M, Rosenthal PJ. 2006. Falstatin, a cysteine protease inhibitor of *Plasmodium falciparum*, facilitates erythrocyte invasion. *PLoS Pathog.* 2:e117. doi:10.1371/journal.ppat.0020117.
- LaCrue AN, Sivaguru M, Walter MF, Fidock DA, James AA, Beerntsen BT. 2006. A ubiquitous *Plasmodium* protein displays a unique surface labeling pattern in sporozoites. *Mol. Biochem. Parasitol.* 148:199–209.
- Rennenberg A, Lehmann C, Heitmann A, Witt T, Hansen G, Nagarajan K, Deschermeier C, Turk V, Hilgenfeld R, Heussler VT. 2010. Exoerythrocytic *Plasmodium* parasites secrete a cysteine protease inhibitor involved in sporozoite invasion and capable of blocking cell death of host hepatocytes. *PLoS Pathog.* 6:e1000825. doi:10.1371/journal.ppat.1000825.
- Pei Y, Miller JL, Lindner SE, Vaughan AM, Torii M, Kappe SH. 2013. *Plasmodium yoelii* inhibitor of cysteine proteases is exported to exomembrane structures and interacts with yoelipain-2 during asexual blood-stage development. *Cell. Microbiol.* 15:1508–1526.
- Huang R, Que X, Hirata K, Brinen LS, Lee JH, Hansell E, Engel J, Sajid M, Reed S. 2009. The cathepsin L of *Toxoplasma gondii* (TgCPL) and its endogenous macromolecular inhibitor, toxostatin. *Mol. Biochem. Parasitol.* 164:86–94.
- Besteiro S, Coombs GH, Mottram JC. 2004. A potential role for ICP, a leishmanial inhibitor of cysteine peptidases, in the interaction between host and parasite. *Mol. Microbiol.* 54:1224–1236.
- Santos CC, Sant’Anna C, Terres A, Cunha-e-Silva NL, Scharfstein J, de A Lima AP. 2005. Chagasin, the endogenous cysteine-protease inhibitor of *Trypanosoma cruzi*, modulates parasite differentiation and invasion of mammalian cells. *J. Cell Sci.* 118:901–915.
- Janse CJ, Franke-Fayard B, Mair GR, Ramesar J, Thiel C, Engelmann S, Matuschewski K, van Gemert GJ, Sauerwein RW, Waters AP. 2006. High efficiency transfection of *Plasmodium berghei* facilitates novel selection procedures. *Mol. Biochem. Parasitol.* 145:60–70.
- Vanderberg JP. 1974. Studies on the motility of *Plasmodium* sporozoites. *J. Protozool.* 21:527–537.
- Matuschewski K. 2006. Getting infectious: formation and maturation of *Plasmodium* sporozoites in the *Anopheles* vector. *Cell. Microbiol.* 8:1547–1556.
- Ghosh AK, Jacobs-Lorena M. 2009. *Plasmodium* sporozoite invasion of the mosquito salivary gland. *Curr. Opin. Microbiol.* 12:394–400.
- Ejigiri I, Ragheb DR, Pino P, Coppi A, Bennett BL, Soldati-Favre D, Sinnis P. 2012. Shedding of TRAP by a rhomboid protease from the malaria sporozoite surface is essential for gliding motility and sporozoite infectivity. *PLoS Pathog.* 8:e1002725. doi:10.1371/journal.ppat.1002725.
- Yoshida N, Potocnjak P, Nussenzweig V, Nussenzweig RS. 1981. Biosynthesis of Pb44, the protective antigen of sporozoites in *Plasmodium berghei*. *J. Exp. Med.* 154:1225–1236.
- Janse CJ, Kroeze H, van Wigcheren A, Mededovic S, Fonager J, Franke-Fayard B, Waters AP, Khan SM. 2011. A genotype and phenotype database of genetically modified malaria-parasites. *Trends Parasitol.* 27:31–39.
- Dua M, Raphael P, Sijwali PS, Rosenthal PJ, Hanspal M. 2001. Recombinant falcipain-2 cleaves erythrocyte membrane ankyrin and protein 4.1. *Mol. Biochem. Parasitol.* 116:95–99.
- Hanspal M, Dua M, Takakuwa Y, Chishti AH, Mizuno A. 2002. *Plasmodium falciparum* cysteine protease falcipain-2 cleaves erythrocyte membrane skeletal proteins at late stages of parasite development. *Blood* 100:1048–1054.
- Rodriguez MH, de la Hernandez-Hernandez F. 2004. Insect-malaria parasites interactions: the salivary gland. *Insect Biochem. Mol. Biol.* 34:615–624.
- Korochkina S, Barreau C, Pradel G, Jeffery E, Li J, Natarajan R, Shabanowitz J, Hunt D, Frevert U, Vernick KD. 2006. A mosquito-specific protein family includes candidate receptors for malaria sporozoite invasion of salivary glands. *Cell. Microbiol.* 8:163–175.
- Ghosh AK, Devenport M, Jethwaney D, Kalume DE, Pandey A, Anderson VE, Sultan AA, Kumar N, Jacobs-Lorena M. 2009. Malaria parasite invasion of the mosquito salivary gland requires interaction between the *Plasmodium* TRAP and the *Anopheles* saglin proteins. *PLoS Pathog.* 5:e1000265. doi:10.1371/journal.ppat.1000265.
- Pimenta PF, Touray M, Miller L. 1994. The journey of malaria sporozoites in the mosquito salivary gland. *J. Eukaryot. Microbiol.* 41:608–624.
- Frischknecht F, Baldacci P, Martin B, Zimmer C, Thiberge S, Olivio-Marin JC, Shorte SL, Ménard R. 2004. Imaging movement of malaria

- parasites during transmission by *Anopheles* mosquitoes. *Cell. Microbiol.* 6:687–694.
46. Steinbuechel M, Matuschewski K. 2009. Role for the *Plasmodium* sporozoite-specific transmembrane protein S6 in parasite motility and efficient malaria transmission. *Cell. Microbiol.* 11:279–288.
 47. Engelmann S, Silvie O, Matuschewski K. 2009. Disruption of *Plasmodium* sporozoite transmission by depletion of sporozoite invasion-associated protein 1. *Eukaryot. Cell* 8:640–648.
 48. Doolan DL, Mu Y, Unal B, Sundaresh S, Hirst S, Valdez C, Randall A, Molina D, Liang X, Freilich DA, Oloo JA, Blair PL, Aguiar JC, Baldi P, Davies DH, Felgner PL. 2008. Profiling humoral immune responses to *P. falciparum* infection with protein microarrays. *Proteomics* 8:4680–4694.
 49. Cohen J, Nussenzweig V, Vekemans J, Leach A, Leach A. 2010. From the circumsporozoite protein to the RTS,S candidate vaccine. *Hum. Vaccin.* 6:90–96.
 50. Agnandji ST, Lell B, Soulanoudjingar SS, Fernandes JF, Abossolo BP, Conzelmann C, Methogo BG, Doucka Y, Flamen A, Mordmüller B, Issifou S, Kremsner PG, Sacarlal J, Aide P, Lanaspá M, Aponte JJ, Nhamuave A, Quelhas D, Bassat Q, Mandjate S, Macete E, Alonso P, Abdulla S, Salim N, Juma O, Shomari M, Shubis K, Machera F, Hamad AS, Minja R, Mtoro A, Sykes A, Ahmed S, Urassa AM, Ali AM, Mwangoka G, Tanner M, Tinto H, D'Alessandro U, Sorgho H, Valea I, Tahita MC, Kaboré W, Ouédraogo S, Sandrine Y, Guiguemdé RT, Ouédraogo JB, Hamel MJ, Kariuki S, Odero C, Oneko M, Otieno K, Awino N, Omoto J, Williamson J, Muturi-Kioi V, Laserson KF, Slutsker L, Otieno W, Otieno L, Nekoye O, Gondi S, Otieno A, Ogutu B, Wasuna R, Owira V, Jones D, Onyango AA, Njuguna P, Chilengi R, Akoo P, Kerubo C, Gitaka J, Maingi C, Lang T, Olotu A, Tsofa B, Bejon P, Peshu N, Marsh K, Owusu-Agyei S, Asante KP, Osei-Kwakye K, Boahen O, Ayamba S, Kayan K, Owusu-Ofori R, Dosoo D, Asante I, Adjei G, Adjei G, Chandramohan D, Greenwood B, Lusingu J, Gesase S, Malabeja A, Abdul O, Kilavo H, Mahende C, Liheluka E, Lemnge M, Theander T, Drakeley C, Ansong D, Agbenyega T, Adjei S, Boateng HO, Rettig T, Bawa J, Sylverken J, Sambian D, Agyekum A, Owusu L, Martinson F, Hoffman I, Mvalo T, Kamthunzi P, Nkomo R, Msika A, Jumbe A, Chome N, Nyakuipa D, Chintedza J, Ballou WR, Bruls M, Cohen J, Guerra Y, Jongert E, Lapiere D, Leach A, Lievens M, Ofori-Anyinam O, Vekemans J, Carter T, Leboulleux D, Loucq C, Radford A, Savarese B, Schellenberg D, Sillman M, Vansadia P, RTS,S Clinical Trials Partnership. 2011. First results of phase 3 trial of RTS,S/AS01 malaria vaccine in African children. *N. Engl. J. Med.* 365:1863–1875.
 51. Agnandji ST, Lell B, Fernandes JF, Abossolo BP, Methogo BGNO, Kawende AL, Kabwende AL, Adegnikaa AA, Mordmüller B, Issifou S, Kremsner PG, Sacarlal J, Aide P, Lanaspá M, Aponte JJ, Machevo S, Acacio S, Buló H, Sigauque B, Macete E, Alonso P, Abdulla S, Salim N, Minja R, Mpina M, Ahmed S, Ali AM, Mtoro AT, Hamad AS, Mutani P, Tanner M, Tinto H, D'Alessandro U, Sorgho H, Valea I, Bihoun B, Guiraud I, Kaboré B, Sombié O, Guiguemdé RT, Ouédraogo JB, Hamel MJ, Kariuki S, Oneko M, Odero C, Otieno K, Awino N, McMorrow M, Muturi-Kioi V, Laserson KF, Slutsker L, Otieno W, Otieno L, Otsyula N, Gondi S, Otieno A, Owira V, Oguk E, Odongo G, Woods JB, Ogutu B, Njuguna P, Chilengi R, Akoo P, Kerubo C, Maingi C, Lang T, Olotu A, Bejon P, Marsh K, Mwambingu G, Owusu-Agyei S, Asante KP, Osei-Kwakye K, Boahen O, Dosoo D, Asante I, Adjei G, Kwara E, Chandramohan D, Greenwood B, Lusingu J, Gesase S, Malabeja A, Abdul O, Mahende C, Liheluka E, Malle L, Lemnge M, Theander TG, Drakeley C, Ansong D, Agbenyega T, Adjei S, Boateng HO, Rettig T, Bawa J, Sylverken J, Sambian D, Sarfo A, Agyekum A, Martinson F, Hoffman I, Mvalo T, Kamthunzi P, Nkomo R, Tembo T, Tegha G, Tsidya M, Kilembe J, Chawinga C, Ballou WR, Cohen J, Guerra Y, Jongert E, Lapiere D, Leach A, Lievens M, Ofori-Anyinam O, Olivier A, Vekemans J, Carter T, Kaslow D, Leboulleux D, Loucq C, Radford A, Savarese B, Schellenberg D, Sillman M, Vansadia P. 2012. A phase 3 trial of RTS,S/AS01 malaria vaccine in African infants. *N. Engl. J. Med.* 367:2284–2295.
 52. Vanderberg JP. 1975. Development of infectivity by the *Plasmodium berghei* sporozoite. *J. Parasitol.* 61:43–50.
 53. Potocnjak P, Yoshida N, Nussenzweig RS, Nussenzweig V. 1980. Monovalent fragments (Fab) of monoclonal antibodies to a sporozoite surface antigen (Pb44) protect mice against malarial infection. *J. Exp. Med.* 151:1504–1513.
 54. Rénia L, Miltgen F, Charoenvit Y, Ponnudurai T, Verhave JP, Collins WE, Mazier D. 1988. Malaria sporozoite penetration. A new approach by double staining. *J. Immunol. Methods* 112:201–205.
 55. Sultan AA, Thathy V, Frevert U, Robson KJ, Crisanti A, Nussenzweig V, Nussenzweig RS, Ménard R. 1997. TRAP is necessary for gliding motility and infectivity of *Plasmodium* sporozoites. *Cell* 90:511–522.